On transport properties of Majorana fermions in superconductors: free & interacting

Gnezdilov, N.V.

Chapter 1

Introduction

1.1 Preface

Majorana fermions are *charge neutral* fermionic modes that equal their own antiparticles [1] and originate from a real solution of the complex Dirac equation [2]. Those recently attracted a lot of attention in the context of subgap states in superconductors [3–11]. In superconducting systems, oppositely charged electron and hole quasiparticle excitations can be naturally thought as particle-antiparticle partners. The particle-hole symmetry relates the creation operator of the quasiparticle excitation $\gamma_E^\dagger$ at energy E to its annihilation operator γ_{-E} at the opposite energy. The p-wave superconducting pairing allows for the subgap solutions of the Bogoliubov-De Gennes (BdG) Hamiltonian at $E = 0$ on vortices in two dimensions [3–5, 8] or as the bound states at the ends of a one-dimensional nanowire [6, 9], which makes the superconductor *topologically non-trivial* [10, 12]. These solutions realize Majorana zero modes $\gamma_0^\dagger = \gamma_0$ (often referred to as Majoranas) that obeys the anticommutation relation $\{\gamma_i, \gamma_j\} = 2\delta_{ij}$. It follows from the reality of Majorana zero modes ($\gamma_i^\dagger = \gamma_i$) that *two* of those are needed to encode a *single* complex fermion, so that each Majorana enters as an *equal-weight superposition* of the electron and hole excitations. This results in 2^N degeneracy of the ground state described by $2N$ Majoranas, non-Abelian exchange statistic of the latter ones [4, 5, 13], and makes them especially attractive in the perspective of topological quantum computation [6, 14, 15].

Once Majorana zero modes are stacked together with sufficient overlap, they form a subgap chiral edge Majorana mode. The left panel in Fig.

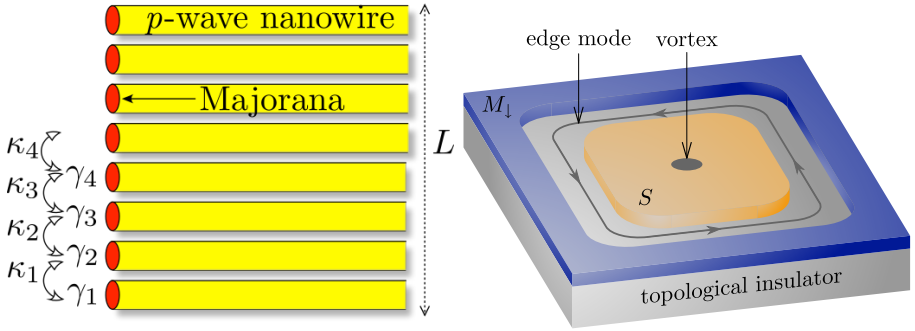

Figure 1.1. *Left panel*: A stack of superconducting nanowires [6] that form a dispersive (see Fig. 1.2) Majorana subgap edge state. The figure is taken from M. Diez, I. C. Fulga, D. I. Pikulin, J. Tworzydło, and C. W. J. Beenakker, New Journal of Physics **16**, 063049 (2014). *Right panel*: 3D topological insulator in proximity to superconductor and ferromagnet hosts Majorana edge mode. The figure is reprinted with permission from A. R. Akhmerov, Johan Nilsson, and C. W. J. Beenakker, Phys. Rev. Lett. **102**, 216404 (2009). Copyright 2009 by the American Physical Society.

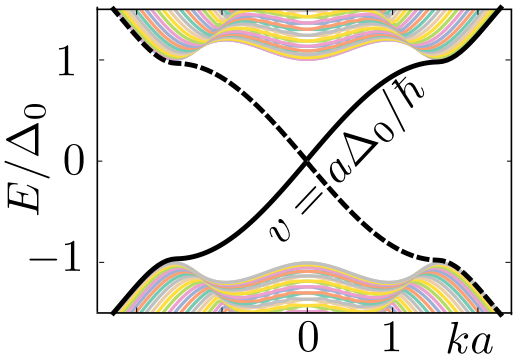

Figure 1.2. Dispersion of a chiral p-wave superconductor drawn from the tight-binding model defined on the infinite stripe geometry (lattice constant a). The bulk of the system is gapped, while the Majorana edge states have the linear dispersion with a slope proportional to the bulk gap Δ_0.

1.1 schematically shows an array of p-wave nanowires [6] that hosts a Majorana edge state. Also, a surface of a three-dimensional topological insulator [10, 16–18] in proximity to superconductor and ferromagnet is predicted to form a Majorana edge mode along the boundary between a ferromagnet and superconductor [19, 20], as it is shown in the right panel

of Fig. 1.1. Moreover, Majorana edge modes at the interface between quantum anomalous Hall insulator and an s-wave superconductor [21] have been recently reported to be observed in experiment [22].

Chiral Majorana edge states in p-wave superconductors with a spin-triplet $p_x + ip_y$ pair potential [4, 7], whose dispersion is shown in Fig 1.2, can be thought as a superconducting analog of chiral edge modes of the quantum Hall effect. However, because Majorana fermions are charge neutral, quantized electrical signatures of the Majorana edge mode are lacking. On the other hand, a temperature gradient is predicted to drive a heat current along the edge carried by Majorana fermions, so that the thermal conductance G is quantized at the electronic quantum $G_0 = \pi^2 k_B^2 T/3h$ times one-half.[1] Study of electrical alternatives to the heat conductance measurements is the goal of Chapters 2 and 3.

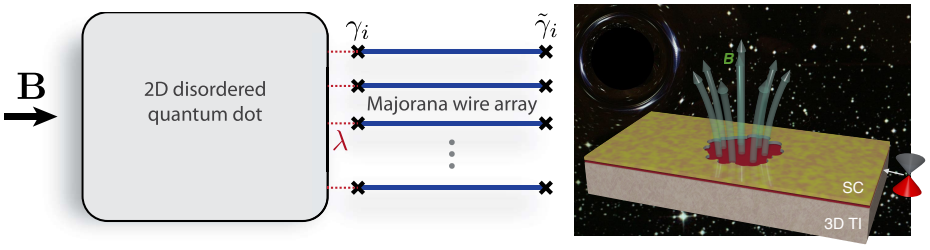

Figure 1.3. *Left panel*: An array of the superconducting nanowires in the magnetic field strongly coupled through a disordered quantum dot. The figure is reprinted with permission from Aaron Chew, Andrew Essin, and Jason Alicea, Phys. Rev. B **96**, 121119(R) (2017). Copyright 2017 by the American Physical Society. *Right panel*: Disordered surface of 3D TI in proximity to a s-wave superconductor in the magnetic field. The figure is reprinted with permission from D. I. Pikulin and M. Franz, Phys. Rev. X **7**, 031006 (2017). Copyright 2017 by the American Physical Society.

The edge states of topological superconductors discussed above are described by the low energy non-interacting theories. In contrast, the second part of the thesis is devoted to the strongly interacting Majorana zero-modes and to the Sachdev-Ye-Kitaev (SYK) model in particular [27, 28]. The interactions are supposed to be so strong, that the quasiparticle description of the model is no longer possible. However, the SYK model is exactly solvable in the large N limit and establishes connections between

[1] The thermal conductance $G = 1/2 \times G_0$ is due to the central charge $c = 1/2$ of the field theory of Majorana edge mode [4, 23–26].

non-Fermi liquids, black hole horizons, and many-body quantum chaos [27, 29, 30].

The SYK model can be realized as a low energy theory of an array of superconducting nanowires in the topological phase [6, 9] once those are strongly coupled through a disordered quantum dot in the magnetic field oriented in the plane of the quantum dot [31]. Additionally, a surface of a three-dimensional topological insulator with an irregular opening in proximity to a superconductor is proposed [32] to be described by the SYK model at low energies (see Fig. 1.3). Chapters 5, 6, and 7 are addressed to direct and indirect transport signatures of the non-quasiparticle nature of the SYK model to characterize these systems.

1.2 Electrical signatures of Majorana surface states

Topological superconductors are analogous to topological insulators [10, 16–18]: Both combine an excitation gap in the bulk with gapless states at the surface, without localization by disorder as long as time-reversal symmetry is preserved. However, the nature of the surface excitations is entirely different: In a topological insulator these are Dirac fermions, relativistic electrons or holes of charge $\pm e$, while a topological superconductor has charge-neutral Majorana fermions on its surface. A transport experiment that aims to detect the Majorana surface states cannot be as routine as electrical conduction — the direct analog for Majorana fermions of the electrical conductance of Dirac fermions is the thermal conductance G_{thermal}. The challenge of low-temperature thermal measurements is one reason why Majorana surface states have not yet been detected in a transport experiment on candidate materials for topological superconductivity [33–37].

There exists a purely electrical alternative to thermal detection of Majorana fermions [38]. Particle-hole symmetry enforces that a Majorana fermion at the Fermi level is an equal-weight electron-hole superposition, so while the average charge is zero, the charge fluctuations have a quantized variance of

$$\operatorname{Var} Q = \tfrac{1}{2}(+e)^2 + \tfrac{1}{2}(-e)^2 = e^2. \tag{1.1}$$

Quantum fluctuations of the charge can be detected electrically in a shot noise measurement. For a single fully transmitted Majorana mode particle hole symmetry enforces a one-to-one relationship between the zero

temperature shot noise power P and the thermal conductance,

$$P/P_0 = G/G_0 = \tfrac{1}{2}\,\mathrm{Tr}\, tt^\dagger, \quad P_0 = e^3V/h, \tag{1.2}$$

where t is the rank-one transmission matrix between two contacts along the edge (biased at voltage $V > 0$, see Fig. 1.4). By definition [2] [39, 40],

$$P = \int_{-\infty}^{\infty} dt\, \langle \delta I(0)\delta I(t)\rangle = \tau^{-1}\,\mathrm{Var}\, Q, \tag{1.3}$$

the shot noise power is the correlator of the current fluctuations and gives the variance of the charge transferred between the contacts in a time τ. Eq. (1.2) implies that $\mathrm{Var}\, Q$ has the universal value $\frac{1}{2}P_0\tau$ for a fully transmitted Majorana mode. These produce a quantized shot noise power P of $\frac{1}{2}e^2/h$ per eV of applied bias [38]. The factor 1/2 reminds us that a Majorana fermion is "half a Dirac fermion".

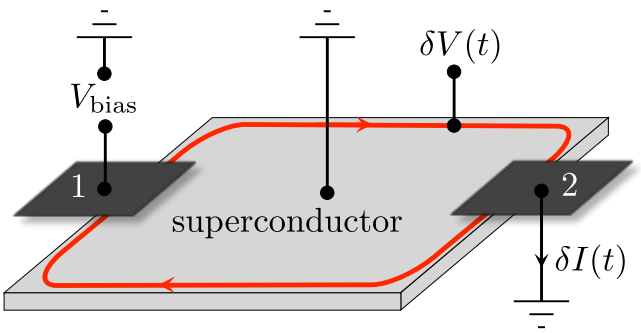

Figure 1.4. Nonlocal current and voltage measurement to detect the charge-neutral Majorana edge mode in a two-dimensional topological superconductor. A bias voltage V excites the edge mode, producing a fluctuating current $\delta I(t)$ and voltage $\delta V(t)$, detected at a remote contact. Because the bulk of the superconductor is grounded, these nonlocal signals are evidence for conduction by gapless edge excitations.

In Chapter 3 of this thesis, we extend the shot noise quantization to the higher moments of charge fluctuations of a single Majorana edge-mode. We explore the relation between the thermal conductance and electrical

[2] The dissipated power in a contact resistance $R = 1/G$, measured in a frequency band width Δf, equals $P_{\mathrm{diss}} = 2RP\Delta f$. To avoid the factor of two, an alternative definition of P has a factor of two in front of the integral in Eq. (1.3). With our definition, the Johnson-Nyquist formula for thermal noise is $P_{\mathrm{thermal}} = 2k_{\mathrm{B}}TG$, while $P_{\mathrm{diss}} = 4k_{\mathrm{B}}T\Delta f$.

shot noise for the *surface* of a three-dimensional topological superconductor in Chapter 2.

1.3 The Sachdev-Ye-Kitaev model in solid state systems

The extreme case of strongly-correlated Majorana zero-modes is under scrutiny in the second part of the thesis. We are going to be focused on the SYK model, which describes N Majoranas with randomized infinite-range interaction in $0+1$ dimensions. It was proposed by Kitaev [27] as a simplified version of the disordered quantum Heisenberg model studied earlier by Sachdev and Ye [28], so that the system would not have a replica symmetry breaking [41, 42] in the large N limit [43, 44]. The SYK Hamiltonian [27, 29, 30] reads

$$H = \frac{1}{4!} \sum_{i,j,k,l=1}^{N} J_{ijkl} \gamma_i \gamma_j \gamma_k \gamma_l \,, \tag{1.4}$$

where γ_i are Majorana zero-modes: $\gamma_i^\dagger = \gamma_i$ and $\{\gamma_i, \gamma_j\} = 2\delta_{ij}$. The couplings J_{ijkl} can be drawn independently from Gaussian distribution with zero mean $\overline{J_{ijkl}} = 0$ and finite variance $\overline{J_{ijkl}^2} = 3!J^2/N^3$.

The SYK model comprises several perculiar properties [27, 29, 30]:

1. it possesses an exact large N solution at *strong* coupling J lacking quasiparticles;

2. emergent conformal symmetry in the infrared;

3. it saturates the upper bound on quantum chaos [45], which is also the case for holographic duals of black hole horizons [46].

Both 1 and 2 can be understood in terms of two-point Green's function found in the long time limit $1 \ll J\tau \ll N$:

$$G(\tau, \tau') = -N^{-1} \sum_{i=1}^{N} \langle \mathcal{T} \gamma_i(\tau) \gamma_i(\tau') \rangle = -\left(4\pi J^2\right)^{-1/4} \frac{\operatorname{sgn}(\tau - \tau')}{\sqrt{|\tau - \tau'|}} \,. \tag{1.5}$$

In frequency representation, the Green's function (1.5) scales as a power-law $1/\sqrt{\omega}$, that has a branch cut rather then quasiparticle like pole struc-

ture. The result (1.5) originates from the solution of a saddle-point equation:

$$J^2 \int d\tau' G(\tau,\tau') G(\tau',\tau'')^3 = -\delta(\tau-\tau'')\,. \tag{1.6}$$

Equation (1.6) remains invariant under time reparametrization $\tau \mapsto f(\tau)$:

$$G(\tau,\tau') \mapsto \left[\partial_\tau f(\tau)\partial_{\tau'} f(\tau')\right]^{\Delta} G\left(f(\tau), f(\tau')\right)\,, \tag{1.7}$$

where $f(\tau)$ is an arbitrary monotonic differentiable function due to the conformal invariance and $\Delta = 1/4$ is an anomalous fermionic scaling dimension [27, 29, 30, 47]. The absence of quasiparticles in the SYK model qualitatively describes the strange metal phase, that exists above the critical temperature in high-T_c superconductors [48, 49], including linear in temperature resistivity in the case of one-dimensional extension of the SYK model [50].

The property of maximal chaos 3 in the SYK model is usually formulated in terms of the so-called Out-Of-Time-Order-Correlation function (OTOC), first introduced by Larkin and Ovchinnikov [51]. It shows how fast the perturbation at time $t = 0$ given by the operator $V(0)$ spreads through the system to influence the later measurement $W(t)$ [45, 52]:

$$F(t) = \mathrm{Tr}\left(\mathrm{e}^{-\beta H}\left[W(t), V(0)\right]^2\right)\,. \tag{1.8}$$

It was recently shown by Maldacena, Shenker, and Stanford [45], that for a many-body quantum system OTOC can not grow faster then exponentially with a characteristic time-scale $t_L \geq \hbar/\left(2\pi k_B T\right)$ known as the Lyapunov time. The SYK model (1.4) is very nonlocal: All degrees of freedom are strongly coupled among each other. This leads to the exponential growth of the OTOC function [27, 29, 30]:

$$\sum_{i,j} \langle \gamma_i(0)\gamma_j(t)\gamma_i(0)\gamma_j(t)\rangle \propto \mathrm{e}^{\lambda_L t}\,, \tag{1.9}$$

that precisely saturates the upper bound on the Lyapunov time $\lambda_L = 1/t_L = 2\pi k_B T/\hbar$ [45]. This is why the SYK model is often refereed as a maximal scrambler.

A possibility to study all these intriguing properties in physical observables inspired a few proposals of realizing the SYK model in a condensed matter platform as a low-energy effective description of an interacting

quantum system [31, 32, 53–55]. The SYK model with Majorana (real) zero-modes is claimed to be a low-energy theory of the Fu-Kane superconductor [8] in a magnetic field with a disordered opening [32], whereas Ref. [31] suggests to use N Majorana nanowires [9] coupled through a disordered quantum dot.

In Ref. [53] Chen *et al* suggested to use a graphene flake to realize the SYK model with the conventional (complex) fermionic zero-modes [3] (cSYK model) [47]:

$$H = \sum_{i,j,k,l=1}^{N} J_{ij;kl}\, c_i^\dagger c_j^\dagger c_k c_l \,, \tag{1.10}$$

where the couplings are hermitian and antisymmetric $J_{ij;kl} = J^*_{kl;ij} = -J_{ji;kl} = -J_{ij;lk}$. Graphene in a perpendicular magnetic field B is known to have Landau levels [57], which are quantized as $E_n \simeq \hbar v\sqrt{2n\, eB/\hbar c}$ with integer n. The 0th Landau level is degenerate [4] and robust [58] under disorder unless the chiral symmetry is broken. Thus, one gets fermionic zero-modes separated from the higher bands by the gap controlled by the magnetic field. As those are robust under disorder, the authors propose to make the boundary of the flake sufficiently irregular. This would make the wave functions of 0th Landau levels $\Phi_i(\mathbf{r})$ random in the real space. Inclusion of the Coulomb interaction $V(\mathbf{r}-\mathbf{r}')$ would enable one to project the interaction term on the basis of 0th Landau levels, so that the projection is governed by the following overlap:

$$J_{ij;kl} = \int d\mathbf{r} \int d\mathbf{r}'\, \Phi_i^*(\mathbf{r})\Phi_j^*(\mathbf{r}')V(\mathbf{r}-\mathbf{r}')\Phi_k(\mathbf{r})\Phi_l(\mathbf{r}')\,, \tag{1.11}$$

that makes the low-energy theory zero dimensional [5] with the cSYK effective Hamiltonian (1.10). The comparison of the generated overlap to

[3] The features of the SYK model mentioned in Section 1.3 are valid for both models with real (Majorana) and complex fermions. The difference is that for the cSYK model the two-point function (1.5) contains the asymmetry parameter of the non-Fermi liquid [56] if the system is away from the charge neutrality point (chemical potential $\neq 0$). We briefly address this issue in the Appendix of Chapter 5. Another distinction between Dirac and Majorana cases is that the right hand side of the reparametrisation prescription (1.7) for complex fermions is multiplied by $g(\tau)/g(\tau')$, where the function $g(\tau)$ appears because of $U(1)$ gauge invariance [47].

[4] Degeneracy of 0th Landau level is proportional to the amount of magnetic flux that flows through the system.

[5] The system can be thought as a strongly interacting disordered *quantum dot*.

the expected Gaussian distribution is shown in Fig 1.5. It is stated that the cSYK model well describes the low-energy theory of the disordered graphene flake of the characteristic size $l \simeq 0.15$ μm that hosts $N \simeq 100$ zero-modes at field strength $B \sim 20$ T [53]. Another proposal for realization of the cSYK model (1.10) with ultracold gases was made by Danshita *et al* [54]. However, all the proposals require for a large number of stable fermionic zero modes separated from the higher bands with a notable gap, sufficient amount of disorder in the system to randomize the wave functions of the zero-modes in the real space, and dominating two-body interaction to be projected on the basis of zero-modes.

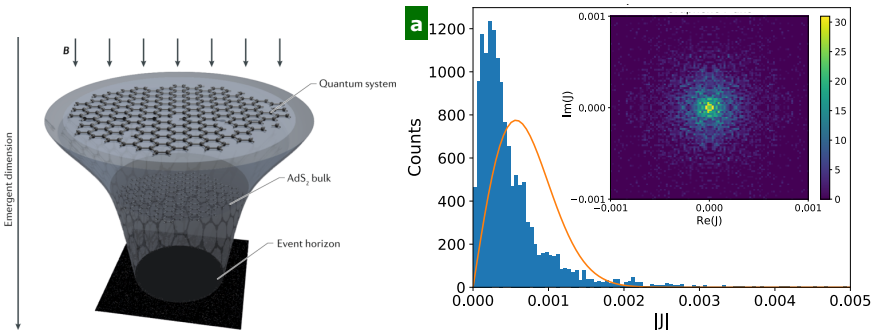

Figure 1.5. *Left panel*: *Holography in a lab.* Strongly interacting disordered graphene quantum dot described by $0+1$-dimensional cSYK model (1.10) at the boundary of $1+1$-dimensional anti-de Sitter space with a black hole [55]. The figure is reprinted by permission from Springer Nature: Marcel Franz and Moshe Rozali, Nature Reviews Materials **3**, 491–501 (2018). Copyright 2018 by Springer Nature. *Right panel*: Statistics of the effective coupling $J_{ij;jk}$ (1.11) for the disordered graphene flake. The figure is reprinted with permission from Anffany Chen, R. Ilan, F. de Juan, D. I. Pikulin, and M. Franz, Phys. Rev. Lett. **121**, 036403 (2018). Copyright 2018 by the American Physical Society.

To characterize the "black hole on a chip" discussed in Refs. [31, 32, 53] propose to measure the local density of states of the SYK quantum dot in a tunneling spectroscopy. The differential tunneling conductance at weak coupling

$$G = \frac{dI}{dV} \propto \mathrm{Im} G^R(V) \propto V^{-1/2} \tag{1.12}$$

reproduces the scaling of the SYK saddle-point solution (1.5) for the voltages in the range of $J/N \ll V \ll J$. The scaling of the differential

conductance (1.5) reveals the emergent conformal symmetry of the SYK model.

1.4 This thesis

Bellow, I briefly highlight the main results presented in the thesis.

1.4.1 Chapter 2

In the first chapter we compare the thermal conductance G_{thermal} (at temperature T) and the electrical shot noise power P_{shot} (at bias voltage $V \gg k_{\text{B}}T/e$) of Majorana fermions on the two-dimensional surface of a three-dimensional topological superconductor. We present analytical and numerical calculations to demonstrate that, for a local coupling between the superconductor and metal contacts, $G_{\text{thermal}}/P_{\text{shot}} = \mathcal{L}T/eV$ (with $\mathcal{L}$ the Lorenz number). This relation is ensured by the combination of electron-hole and time-reversal symmetries, irrespective of the microscopics of the surface Hamiltonian, and provides for a purely electrical way to detect the charge-neutral Majorana surface states. A surface of aspect ratio $W/L \gg 1$ has the universal shot-noise power $P_{\text{shot}} = (W/L) \times (e^2/h) \times (eV/2\pi)$.

1.4.2 Chapter 3

It was found in Ref. [38], that the Majorana fermions propagating along the edge of a topological superconductor with $p_x + ip_y$ pairing deliver a shot noise power of $\frac{1}{2} \times e^2/h$ per eV of voltage bias. In this chapter we calculate the full counting statistics of the transferred charge and find that it becomes trinomial in the low-temperature limit, distinct from the binomial statistics of charge-e transfer in a single-mode nanowire or charge-$2e$ transfer through a normal-superconductor interface. All even-order correlators of current fluctuations have a universal quantized value, insensitive to disorder and decoherence. These electrical signatures are experimentally accessible, because they persist for temperatures and voltages large compared to the Thouless energy.

1.4.3 Chapter 4

There exists an analogy of topological superconductors reveals while considering graphene superlattice shown in Fig. 1.6. Dirac electrons in

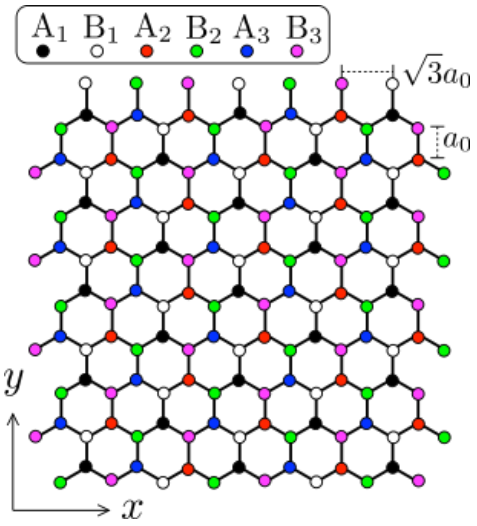

Figure 1.6. Graphene superlattice with a periodic potential modulation. Different colors distinguish the carbon atoms on the A and B sublattice, each of which has an ionic potential V_{A_n}, V_{B_n}, $n = 1, 2, 3$, induced by the substrate.

graphene have a valley degree of freedom that is being explored as a carrier of information. In that context of "valleytronics" one seeks to coherently manipulate the valley index. In this chapter we show that reflection from a superlattice potential can provide a valley switch: Electrons approaching a pristine-graphene–superlattice-graphene interface near normal incidence are reflected in the opposite valley. We identify the topological origin of this valley switch, by mapping the problem onto that of Andreev reflection from a topological superconductor, with the electron-hole degree of freedom playing the role of the valley index. The valley switch is ideal at a symmetry point of the superlattice potential, but remains close to 100% in a broad parameter range.

1.4.4 Chapter 5

In this chapter we study how the non-Fermi liquid behavior of the closed system in equilibrium manifests itself in an open system out of equilib-

rium. We calculate the current-voltage characteristic of a quantum dot, described by the complex-valued SYK model, coupled to a voltage source via a single-channel metallic lead (coupling strength Γ). A one-parameter scaling law appears in the large-N conformal regime, where the differential conductance $G = dI/dV$ depends on the applied voltage only through the dimensionless combination $\xi = eVJ/\Gamma^2$. Low and high voltages are related by the duality $G(\xi) = G(\pi/\xi)$. This provides for an unambiguous signature of the conformal symmetry in tunneling spectroscopy.

1.4.5 Chapter 6

We study the observable properties of quantum systems which involve a quantum continuum as a subpart. We show in a very general way that in any system, which consists of at least two isolated states coupled to a continuum, the spectral function of one of the states exhibits an isolated zero at the energy of the other state. Several examples of quantum systems exhibiting such isolated zeros are discussed. Although very general, this phenomenon can be particularly useful as an indirect detection tool for the continuum spectrum in the lab realizations of quantum critical behavior.

1.4.6 Chapter 7

In this chapter we demonstrate that a single fermion quantum dot acquires odd-frequency Gor'kov anomalous averages in proximity to strongly correlated Majorana zero-modes, described by the SYK model. Despite the presence of finite anomalous pairing, superconducting gap vanishes for the intermediate coupling strength between the quantum dot and Majoranas. The increase of the coupling leads to smooth suppression of the original quasiparticles.

1.4.7 Chapter 8

In the last chapter we consider another model with infinity ranged interaction. We found analytically a first-order quantum phase transition in a Cooper pair box array of N low-capacitance Josephson junctions capacitively coupled to resonant photons in a microwave cavity. The Hamiltonian of the system maps on the extended Dicke Hamiltonian of N spins 1/2 with infinitely coordinated frustrating interaction. This interaction arises from the gauge-invariant coupling of the Josephson-junction phases

to the vector potential of the resonant photons field. In the $N \gg 1$ semi-classical limit, we found a critical coupling at which the ground state of the system switches to one with a net collective electric dipole moment of the Cooper pair boxes coupled to a super-radiant equilibrium photonic condensate. This phase transition changes from the first to second order if the frustrating interaction is switched off. A self-consistently "rotating" Holstein-Primakoff representation for the Cartesian components of the total superspin is proposed, that enables one to trace both the first- and the second-order quantum phase transitions in the extended and standard Dicke models, respectively.